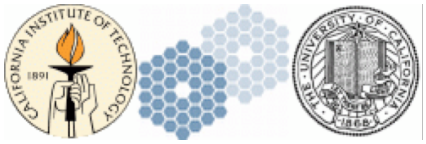

Keck Adaptive Optics Note 685

NGAO Optical Relay Design

Renate Kupke

Revised, Oct 27, 2009

1. Introduction

This document presents the preliminary optical design for the Keck Next Generation Adaptive Optics Relay. The design is based on results of the conceptual design study, KAON 549, and subsequent build-to-cost reductions and guidelines. Section 2 of this document outlines some of the main requirements the optical design must satisfy. Section 3 describes the components of the optical relay in more detail, and in Section 4 the performance of the relay with regard to science instruments and wavefront sensors is discussed.

2. Design Choices and Requirements

The requirements, as defined in KAON 549 for the conceptual design, have altered somewhat due to build-to-cost design changes in KAON 642. The current requirements include, but are not limited to:

- Location:
  - The AO system will reside on the left Nasmyth platform. (SR-744)
- Wavelength Range
  - The AO relay shall transmit a wavelength range of 0.818μ - 2.4μ for the NIR imager (INT 157) and NIR integral field spectrograph (INT-382).
  - The AO relay shall transmit 1.16-1.77μ to the LOWFS (FR-175) and shall not preclude K-band
  - The AO relay shall transmit 1.1-4.1μ to the interferometer (SR-683).
  - The NGS WFS will require 0.4-0.8μ light (FR-140 and KAON 642).
  - THE LGS WFS will require 589nm sodium light (FR-523).
- Field of View:
  - A high Strehl science relay with an unvignetted field of view (FOV) of at least 20 arcseconds diameter with a goal of 40 arcseconds diameter. (FR 41)
  - A 120 arcsecond diameter field of regard (FOR) at the focal plane of the first relay, providing natural guide stars (NGS) for the low-order wavefront sensors (LOWFS). (FR 40)
  - A 120 arcsecond diameter unvignetted FOR for guidestars from 80 to 120km in altitude to the LGS WFS.
- Entrance Window

    - The entrance window shall provide a thermal seal between the cold enclosure of the AO system and the ambient room temperature. It shall consist of two windows to prevent condensation, and it shall be big enough to transmit the entire 120” field of view.
- Field and Pupil Rotation:
    - The optical relay will have a K-mirror upstream of the science instruments and wavefront sensors that can pass the entire field of view.
- Deformable mirrors
    - The wide field relay shall contain a deformable mirror conjugate to the telescope pupil, with a pupil size of 100mm. The deformable mirror shall have 22 actuators across the pupil diameter. (FR-32 and FR-56). The requirements do not state whether this is circumscribed pupil diameter, maximum mirror diameter, active mirror area, or mirror area, so a primary mirror diameter of 10.949m circumscribed mirror diameter is assumed.
    - The narrow field relay shall contain a deformable mirror conjugate to the telescope pupil with a pupil size of 24mm. The deformable mirror shall have 63 actuators across the pupil diameter. (FR-33 and FR-57).
- Output pupil location:
    - The exit pupil for the first relay will be telecentric to simplify design of the LOWFS pick-off mechanisms. (FR-1502)
    - The exit pupil for the entire relay will be telecentric to simplify design of the NGS WFS. (FR-1501)
- Output focal ratio:
    - The output focal ratio of the first relay shall be the same as the input focal ratio of the telescope, and shall be made compatible with the input for the LOWFS, the second relay, the acquisition camera, and the interferometer. (F-1499)
    - The output focal ratio of the second relay shall be greater than f/40 . (FR-1500)
- Optical Switchyard
    - The relay design should provide for a LGS WFS sodium dichroic (FR-67), a removable NGS WFS dichroic (FR-39), and a removable acquisition camera fold (FR-68). There are currently no requirements for instrument selection.

3. First-Order Optical Layout

An annotated optical layout is shown in Figure 1. The following sub-sections describe each component of the optical relay in detail.

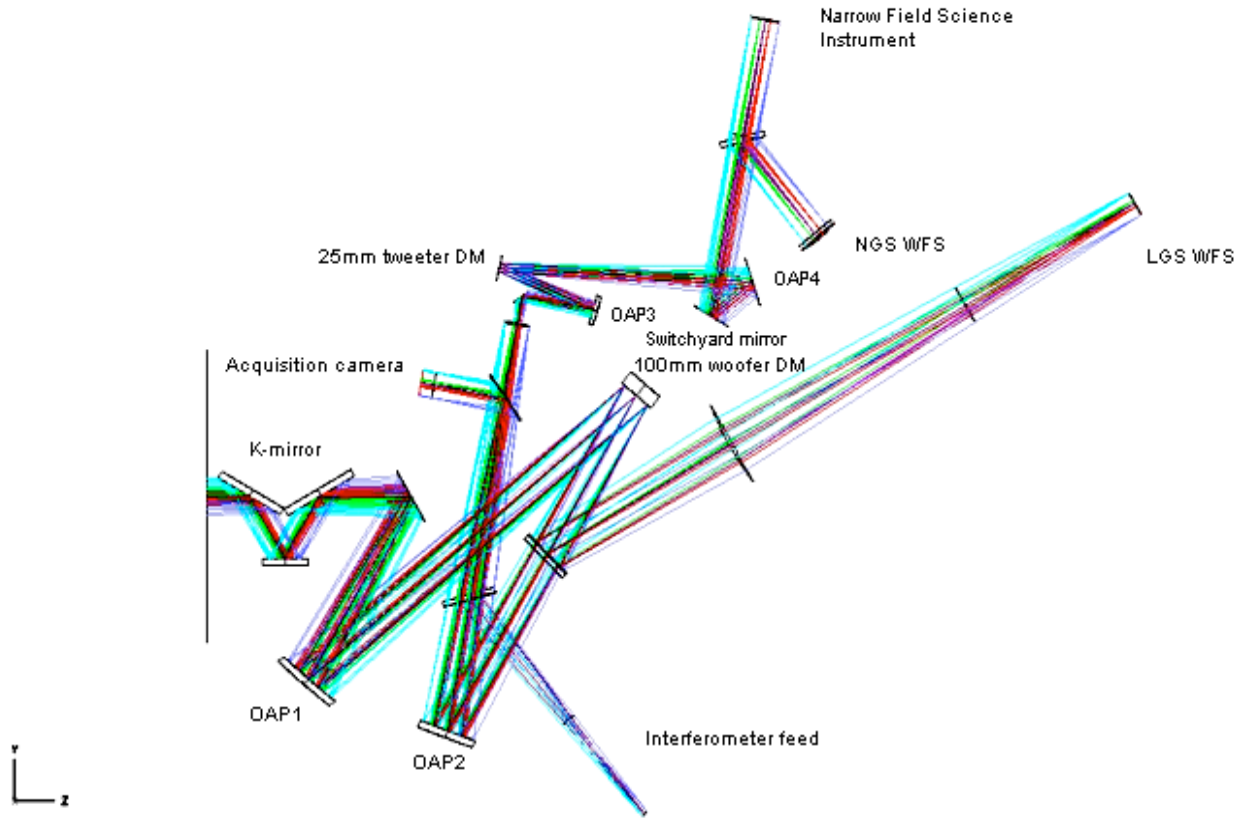

Figure 1 Annotated optical layout of the 1-tier, cascaded relay. Light from the telescope tertiary mirror enters from the left. The first, f/15 matched-OAP relay contains a 100mm woofer DM conjugate to the telescope primary. The second, f/46 OAP relay contains the 25mm MEMs tweeter DM conjugate to the telescope primary. The LGS dichroic picks off laser light, which is directed to the LGS WFS. Pick-offs for the tip-tilt and low-order wavefront sensors (LOWFS) lie at the focal plane of the f/15 relay, and are not shown in this figure. There are also removable dichroic beamsplitters for the interferometer, the acquisition camera, and the natural guide star

3.1. K-mirror rotator

The Nasmyth focus lies between the first and second mirrors of the K-mirror assembly (K1 and K2, respectively). The focal plane is located 121mm after K1. The location of the focus is placed within the K-mirror to provide adequate space for the first off-axis parabola (OAP) of the relay, as described in the next section. The existing Keck AO relay has the first element of the K-mirror positioned after focus. The decision to move the focus to a point within the K-mirror assembly was based on the need to accommodate a smaller woofer DM (100mm versus the existing 140mm diameter), and thus a shorter focal length OAP1.

The K-mirror consists of 3 mirrors, the first and third being tilted at 60 and -60 degrees, respectively, to the Nasmyth optical axis. The tilt angles are identical to the present Keck AO K-

mirror assembly. The mirror diameters (assuming a 90% clear aperture) are as follows: K1=250mm, K2=160mm, and K3=270mm. K1 is slightly larger than the present Keck AO K-mirror's K1 because of the need to pass both the LGS and NGS 120 arcsecond diameter FOV. K2 is the same size as the existing K2, and K3 is slightly smaller. The distance between K1 and K2, and K2 and K3, is 243.5mm, as in the existing Keck image rotator. The mechanical design of the K-mirror assembly can therefore be very similar to that of the existing K-mirror.

3.2. First Relay

The first relay consists of two matched off-axis parabolas, the first of which produces, in collimated space, a plane conjugate to the primary mirror at which the 100mm woofer DM is placed. In the collimated space after the 100mm diameter deformable mirror lies a dichroic designed to reflect laser guide star light (589nm) to the LGS WFS, and transmit all other wavelengths. The second OAP of the matched pair relays the Nasmyth focus to a second focal plane, preserving the f-number of the input beam. In the converging light following OAP2 are removable pick-offs to the interferometer and acquisition cameras.

To accommodate a one tier design, an additional fold mirror is needed in the diverging optical space following the K-mirror. This fold mirror lies 322.5mm after K3, with an incidence angle of 30 degrees and a diameter of 180mm. The present Keck AO relay contains a similar fold mirror, which is used also as a tip-tilt steering mirror. It was decided not to incorporate this fold as a tip-tilt location, as its conjugate location is 22km above the telescope, and a location conjugate to the telescope pupil was preferred to not move the pupil and to lessen the stroke requirement of the tip/tilt stage.

OAP1 has a focal length determined to meet the requirement of a 100mm pupil on the woofer DM by the following equation:

$$F_{OAP} = \left[\frac{d_{DM}}{d_{PM}}\right] F_{tel} \tag{1}$$

where d_{DM} and d_{PM} are the diameters of the deformable mirror (100mm) and the telescope primary (10.949m), respectively, and F_{tel} is the focal length of the telescope (149.583m). This gives a focal length for OAP1 of 1366.2mm.

In an effort to reduce cost the off-axis angles (OAA) of the OAPs have been reduced from 25° to 20° in the preliminary design phase. This also results in slightly less wavefront error in the path of the LGS WFS. This wavefront error results from the LGS location at a finite conjugate, while the relay is optimized for an infinite conjugate (discussed in more detail in section 4). The OAA of 20° results in a decenter of 481.8mm from the center of the parent parabola.

The woofer DM follows OAP1, at a distance from OAP1 conjugate to the telescope primary mirror:

$$t_{OAP1 \to DM} = \left(\frac{-1}{t_{pupil} + F_{OAP1}} + \frac{1}{F_{OAP1}} \right), \tag{2}$$

where t_{pupil} is the distance to the telescope exit pupil from telescope focus. Equation (2) gives a total OAP1 to woofer DM distance of 1460mm.

The woofer DM is nominally 22x22 actuators (5mm pitch), and will be mounted on a real-time, tip-tilt platform. Due to the incident angle of 10° the pupil will be elongated by 1.54%.

In collimated space, 625mm after the woofer deformable mirror, lies the dichroic beamsplitter that will pick off the 589nm light of the sodium LGS and direct them to the LGS WFS. This beamsplitter has an incidence angle of 15° to the optical axis, and a diameter of 200mm.

Following the woofer DM is OAP2, an off-axis parabola whose parameters exactly match those of OAP1 to minimize aberrations at infinite conjugate. It is located one focal length (1366mm) away from the woofer DM, projecting the pupil to infinity and providing a telecentric beam for the second relay and LOWFS relays. A telecentric system was chosen to simplify the design of the LOWFS pick-off mechanisms and wavefront sensors. A telecentric system does not require tilt with field to keep the chief ray constant on entering the wavefront sensor. There are also no pupil scale changes with conjugate distance for the LGS WFS.

3.3. Tip-tilt platform

During the preliminary design stage, inquiries were submitted to vendors regarding the mounting of the woofer deformable mirror on a fast tip-tilt stage. Primarily, we desired a comparison between the performance and cost of mounting a 100mm diameter piezo-electric DM versus the larger 140mm diameter DM. CILAS provided information about the SAM 416 (Gemini 4.5) and the SAM 349 (GTC) deformable mirrors, shown in Table 1. These two mirrors are similar to our requirements for 100mm and 140mm woofer DM.

Table 1 Characteristics of existing CILAS DMs.

DM	# actuators	pitch	aperture	Max stroke PV	weight	volume
SAM 416	416	5.0mm	106mm	7.8μ	6.5kg	15x16x10cm^3
SAM 349	349	7.0mm	140mm	8.4μ	14.4kg	22x22x20cm^3

The mirrors listed in the table above were not intended for mounting on a tip/tilt platform. CILAS estimated that the weight of these DMs could be decreased by as much as 20% by changing the mechanical packaging in consideration of the tip-tilt platform mounting. When contacting the vendors the specifications included a 38.5Hz closed-loop bandwidth (the most stringent tip-tilt bandwidth requirement contained in the science cases), and the ability to compensate for the ~30Hz telescope vibration in an as-yet-unspecified feed-forward fashion. The requirements database indicates a 3 arcsecond stroke is required on the tip/tilt platform (SR 688). At the tip/tilt platform at the woofer DM this corresponds to

$$\alpha_{TT} = \left(\frac{F_{Tel}}{F_{OAP1}} \right) \alpha_{Sky},$$

where α_{Sky} is the 3 arcsecond stroke requirement on the sky, F_{Tel} is the focal length of the telescope and F_{OAP1} is the focal length of OAP1. This results in a α_{TT} of 1.6 milliradians peak-to-peak. Momentum compensation was also required to minimize vibration on the optical table.

Three vendors responded positively: CILAS, Physik Instrumente, and Left-hand Design. The bandwidth requirements, considering the weight and dimensions of the deformable mirror, are challenging. Table 2 summarizes the results of the inquiry. Physik Instrumente and Left Hand design indicated that the 140mm, with its 14.4kg weight, would be difficult to achieve at the specified bandwidth. CILAS, although not giving exact bandwidth values, suggested the 140mm diameter mirror would operate at a 30% decreased bandwidth over the 100mm. For this reason, the 100mm DM was chosen as baseline for the AO relay design.

Table 2 Results of initial vendor inquiries into tip/tilt stage.

	CILAS	PI	Left-hand Design
Predicted achievable bandwidth	? has reached 50Hz for TMT prototype	200Hz resonant frequency, claims 50Hz closed-loop	Open-loop servo control: Phase 1:20Hz, Phase 2: 50Hz, Phase 3 100Hz, Phase 4 200Hz
sensor		Capacitive	
type	Voice coil?	Piezo	Voice coil

3.4. Laser Guide Star WFS

As illustrated in Figure 1, between the woofer DM and OAP2 is a fixed dichroic beamsplitter which will reflect sodium guide star light to the LGS WFS. The dichroic was placed in collimated space to minimize aberrations in the science and LOWFS beams. The LGS WFS does not receive a performance benefit from the matched OAPs due to the finite location of the laser guide star objects, nor do they share the same static aberrations as the science and LOWFS stars, thus no loss in performance or significant increase in calibration complexity is incurred by using a separate focusing element for the laser guide stars.

The dichroic pick-off will ideally be a notch filter, reflecting only the sodium (Na) LGS wavelength of 589nm. A notch filter was chosen to allow visible light below 600nm to be available to the visible truth wavefront sensor (TWFS) located in the LOWFS assembly, and the NGS WFS. The dichroic has an incidence angle of 15°. The optical layout for only the LGS WFS section of the AO relay is shown in Figure 2. Because the LGS WFS dichroic lies downstream of the woofer DM, the LGS WFS will operate in closed-loop.

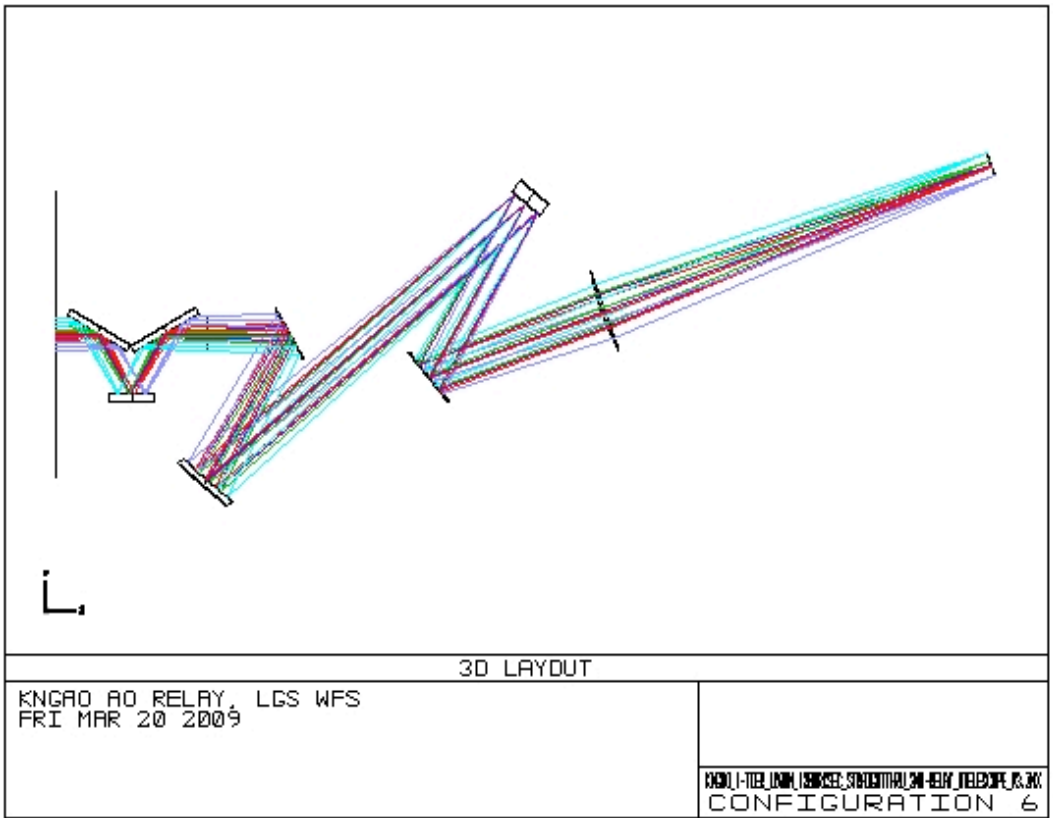

Figure 2 The LGS WFS optical relay.

The object selection mechanism (OSM) for the LGS WFS requires a focal plane, thus the collimated light reflected from the LGS dichroic is brought to focus by a single glass plano-convex lens. Zemax modeling indicates that this lens will produce less wavefront error if the convex surface is a parabola (see figure 3). The radius of curvature of the lens was chosen to maintain the 1:1 magnification of the relay. The lens is located one focal length away from the woofer DM, to provide a telecentric beam for the LGS OSM and relays. The lens will be incorporated into the double pane window of the AO enclosure, as the LGS WFS unit will sit outside of the cold enclosure. +-

In the converging beam following the lens, there is adequate space for a removable mirror providing a 90° reflection to a visible laser guide star acquisition camera if one is desired (this is not planned).

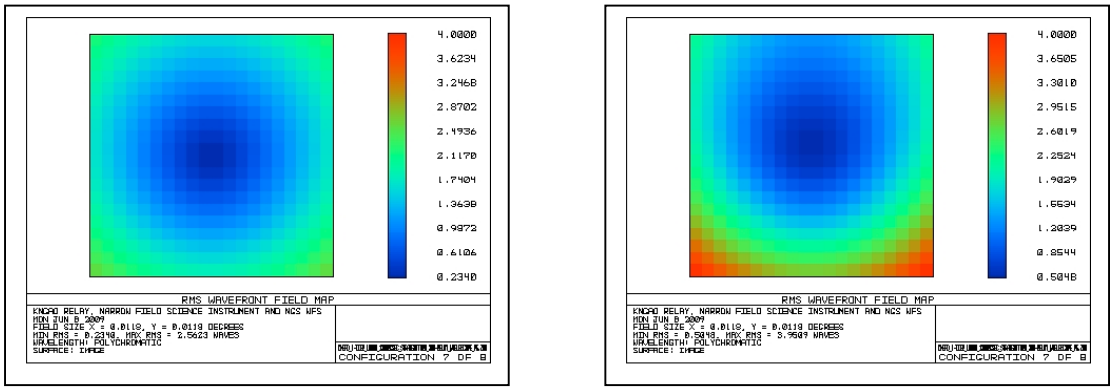

Figure 3 Comparison of RMS wavefront error over the LGS WFS field with a parabolic plano-convex focusing lens (left) and a spherical plano-convex focusing lens (right). Final focal planes are adjusted for tilt and field curvature.

3.5. Interferometer Feed

Located 500mm after OAP2 is a removable dichroic available to feed the Keck interferometer. The interferometer will be used in conjunction with Keck NGAO, and therefore simultaneously with the LOWFS. The interferometer utilizes J and H band light for internal tracking (the J-band used primarily when doing H-band interferometer science). It has therefore been decided that the interferometer dichroic will reflect J, H, K, and longer wavelength light, up to the required 4.1μ, to the interferometer. The LOWFS will be required to perform wavefront sensing at wavelengths below 1μ . The dichroic has an incidence angle of 25° and a diameter of 190mm. A wedge of 0.17° on the second surface of the dichroic removes lateral color over J-band at the LOWFS plane.

The interferometer dichroic directs the starlight to two field-steering mirrors. One of the mirrors has a hole which allows the on-axis light to pass straight through, while off-axis light is directed to the second field selection mirror. Both diverging beams are collimated with OAPs which are identical in diameter, focal length, and off-axis angle to the existing Keck DSM collimating OAPs. They are, however, in a different location. The collimated beams are directed to two steering dichroics, which both direct light to down-looking mirrors feeding the existing Nasmyth interferometer path, and provide light to diagnostic sensors located behind the dichroics. The beams feeding the interferometer will need correction in both path length and polarization in order to match the existing system on the other Keck telescope. The polarization analysis is still to be completed.

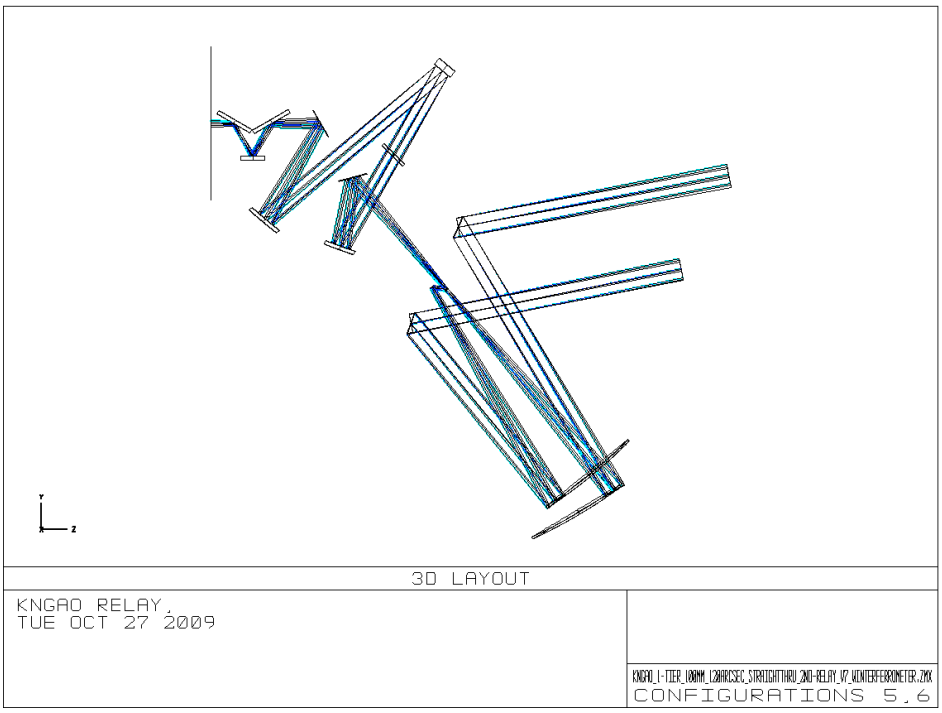

Figure 4 KNGAO relay showing interferometer pick-off, the field selection mirrors, the collimating OAPs and fold dichroics of the Dual Star Module bench.

3.6. Wide-Field Relay to Acquisition Camera and LOWFS.

After the dichroic LGS WFS pick-off, the beam is refocused by OAP2 to produce an f/13.66 focal plane at the LOWFS pick-off plane. Located 250mm before the focal plane is a removable mirror, allowing a 90° reflection to an acquisition camera. The acquisition camera will obtain images of the entire 120 arcsecond diameter field and allow acquisition of the natural guide stars for the LOWFS and an initial acquisition of the LGS. The LOWFS focal plane and acquisition camera pick-off are shown in Figure 5. For the mechanical envelope, we have assumed that the acquisition camera design will be similar to the existing MAGIQ guider camera design, adapted to accommodate a slightly smaller field of view (2 arcminutes versus 3 arcminutes for the existing MAGIQ design). The acquisition camera must translate as a unit (field and camera lenses, as well as detector) to refocus for the LGS acquisition.

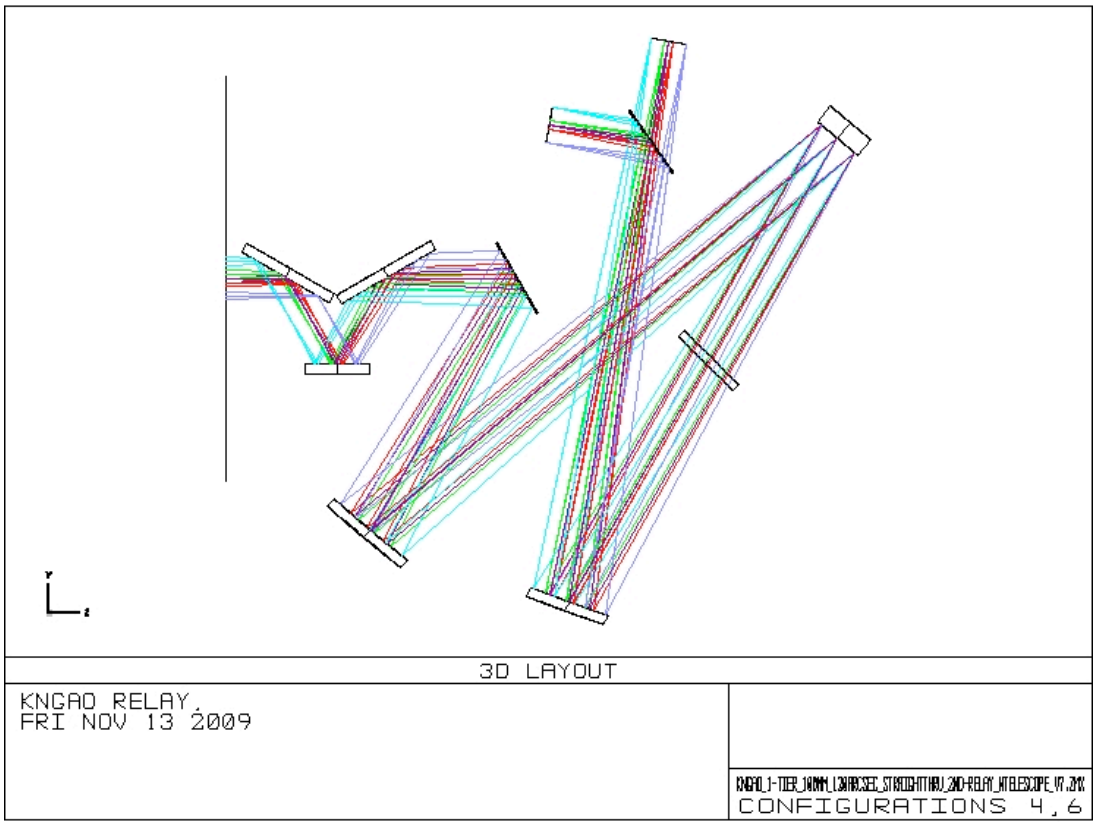

Figure 5 Wide-field relay, passing 120 arcseconds to tip-tilt sensors and low-order wavefront sensors. A removable mirror provides the acquisition camera with the entire 120 arcsecond field of view.

3.7. Narrow-field, High Strehl Relay

Within the plane of the LOWFS pick-offs will be an unobstructed aperture to pass a 40x60 arcsecond rectangular field of view to a narrow-field, high Strehl relay. Although the science instruments require only a 40 arcsecond field of view (FOV), the larger 40x60 arcsecond rectangle was chosen to increase the patrol field of the natural guide star wavefront sensor. The optical path is shown in Figure 6. Directly after the focal plane, a fold mirror directs the light perpendicularly to its original direction to allow space for following optics (specifically the MEMs deformable mirror package) within the LOWFS pick-off mechanisms.

The narrow-field relay of the KNGAO consists of two unmatched OAP mirrors producing a 24mm pupil image on the tweeter DM and an output beam to feed the NIR imager, the integral field spectrograph (IFS), and the natural guide star wavefront sensor (NGS WFS). The tweeter deformable mirror is a 64x64 actuator MEMs device with 0.4mm actuator centers. The tweeter mirror has an incidence angle of 10°. The MEMs device will be mounted on a "slow" tip-tilt stage, as discussed in KAON 669, to provide a steering mirror that can be used for differential tracking, compensation of differential atmospheric refraction, or fine guidance and centering on a

spaxel or detector. The performance requirements of this steering platform are outlined in KAON 669. A specific platform that will accommodate the tight spatial constraints within the LOWFS package has not yet been identified, and remains as work for the PDR.

Using Equation (1), we can determine the focal length of the OAP needed to produce a collimated beam with a 24mm telescope primary image on the tweeter DM (this corresponds to 60x60 subapertures). In this case, we substitute F_{OAP2} for F_{tel} and d_{DM1} for d_{PM}, to get F_{OAP3}=327.9mm. The pupil at the output of the first relay is telecentric, so the tweeter DM lies F_{OAP3} away from OAP3. The requirement FR-1500 dictated a focal ratio greater than f/40 for the beam exiting the relay, in order to provide space for an optical switchyard and instruments. F_{OAP4} is thus 3 times larger than F_{OAP3}, or 987.7mm. This provides an output focal ratio of 3xf/13.66 or f/40.98. OAP4 is located exactly one focal length away from the tweeter mirror, to provide a telecentric beam for the instruments.

A switchyard mirror, at 400mm beyond OAP4, directs the beam to the science instrument(s). The incident angle of the mirror is 20°. Although access to a visitor instrument port is not a requirement of the NGAO relay, this mirror could, in principal, be used to direct the beam to other instrument locations, including below and above the optical plane, or across the LGS WFS beam to an instrument at the location of the movable DSM table. This allows expansion of KNGAO to feed additional instruments in the future.

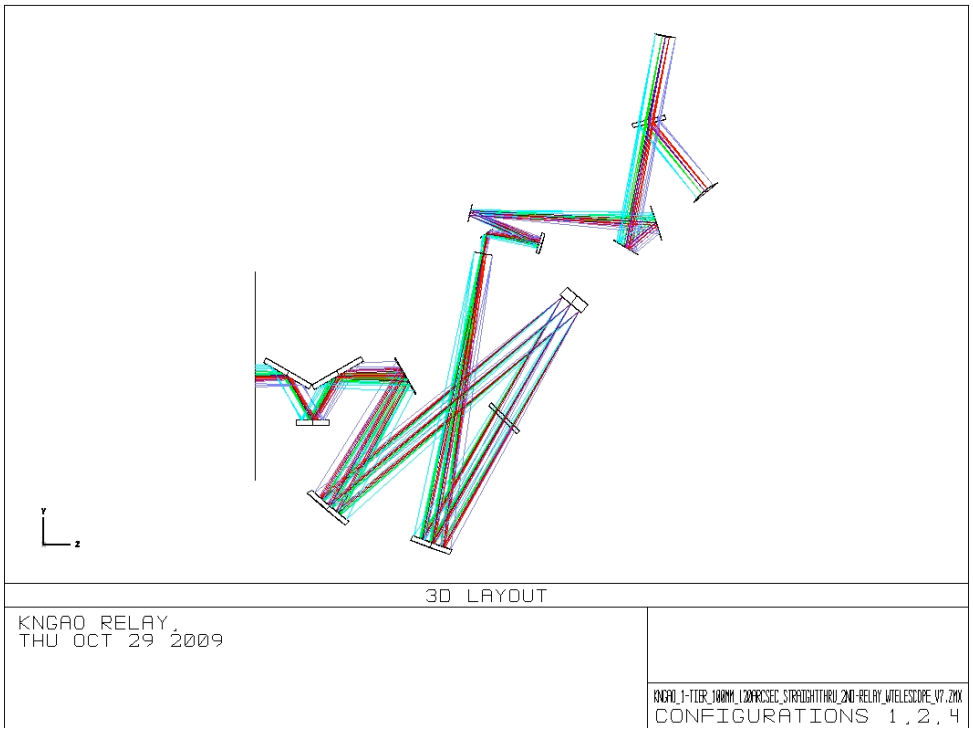

Figure 6 The 40 arcsecond FOV science instruments and NGS WFS are fed by the second OAP relay.

3.8. Natural Guide Star Wavefront Sensor (NGS WFS)

A removable dichroic is located 605mm beyond the switchyard mirror, with an incidence angle of 25°. We are assuming that the NGS WFS will include a pick-off system similar to a single LOWFS pick-off to acquire the guide star, be mounted on a translation stage to acquire the NGS, or alternatively a pair of field steering mirrors will be required. A patrol field larger than the science FOV was desired for the NGS WFS, so the 2nd relay optics were designed to accommodate a rectangular 40x60 arcsecond field. A diagram of the field, and it's relation to the science and LOWFS fields, is shown in figure 7

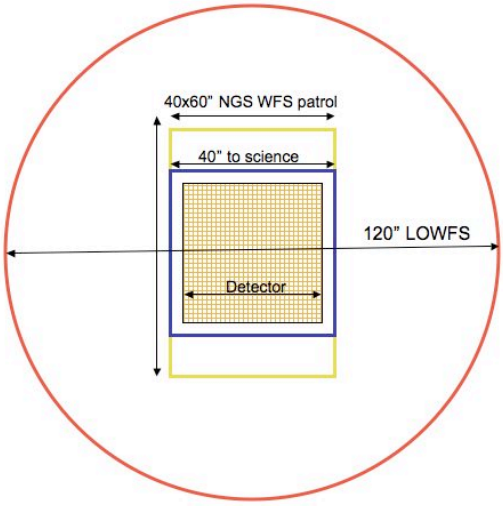

Figure 7 Outline of respective fields of view. The 120" diameter LOWFS patrol field (red), the rectangular 40x60" NGS WFS patrol field (yellow), the 40" field desired for the science instrument (blue) and a representative detector area (orange hatched).

It has also been proposed that the NGS WFS could act as a LOWFS when the observer requires the science object as a wavefront sensor reference in fixed pupil mode (see KAON 666).

3.9. Science Instrument

The NIR instruments are fed directly by the f/41 narrow-field relay output. In the beam between OAP4 and the instrument is one removable dichroic. The dichroic has a wedge angle of 0.4° to correct lateral color at the instrument plane. When the dichroic is removed, the focal position of the beam will shift both laterally and along the optical axis. The lateral shift can be compensated with a re-pointing of the telescope. The shift in focal plane may be removed with a telescope focus adjustment. A 20mm thick dichroic tilted at 25° causes roughly 7mm of focal plane shift. The instrument focal plane has a finite curvature (discussed in the performance section 4.2).

3.10 Science Instrument ADC

An atmospheric dispersion corrector will be required to correct the lateral color introduced by the atmosphere at the science instrument. The corrector need work over the science instrument bandpasses, which include z, y, J, H, and K (see passbands definition document, KAON 554). It is also possible that the science instrument may be required to work at r' and i' bands (down to 620nm).

There are two possible designs for the ADC: a linear ADC, and a counter-rotating prism pair. The linear ADC, as applied to the NGAO project, has been investigated at a cursory level by Brian Baumann in the conceptual design phase. An IR ADC design, by Peter Wizinowich, exists for NIRC2. The linear ADC design has the advantage of fewer surfaces, but requires more physical space than the counter-rotating prisms. If the final science instrument passbands do not include r' and i', an attempt will be made to accommodate the remaining passbands with a single ADC. Otherwise, two exchangeable ADCs will have to be available for either visible or NIR observations.

4. Performance

To determine the performance of the optical system, several sources of optical degradation were analyzed using Zemax in the wavelength passbands used by the science instruments and wavefront sensors. The passbands are defined in KAON 530.

The optical relay was modeled in conjunction with the Keck primary and secondary mirrors, to ascertain the combined effects of the two optical systems.

Field points used were the maximum off-axis fields defined for each instrument. The wavefront errors and RMS spot radii quoted are the worst-case for the field points analyzed.

The working f/# of the wide-field relay is f/13.66 and of the narrow-field relay is f/40.98. Airy disk sizes are defined by

$$r_{airy} = 1.22\lambda F/\# \qquad (3)$$

and the depth of focus (DOF) is defined by $DOF = 4\lambda\left(F/\#\right)^2$.

In the Zemax model, both the woofer and tweeter DMs are represented by Zernike Standard Sag surfaces. This allows correction of wavefront errors in the same way a deformable mirror would compensate for static errors. Coefficients from the Zemax Zernike coefficient analysis tool, converted to mm Sag, were used to determine the magnitude of Zernike aberrations applied to the surface. In most cases the aberration was field dependent, so an effort was made to achieve good performance over the entire field of regard.

Chromatic focal shift and lateral color, where applicable, were evaluated for different wavelength ranges using the Zemax analysis tools. Lateral color and chromatic focal shift arise

only in beam paths in which there are transmissive optics, such as beamsplitters. The effect of the entrance and exit windows has not yet been evaluated, but will be completed for PDR.

4.1 LOWFS

Except in the case of interferometer observations, the only non-reflective optic preceding the LOWFS is the LGS dichroic beamsplitter, which is located in collimated space. Chromatic aberrations over the wavelength range used by the LOWFS are thus very small.

The insertion of the dichroic during interferometer use will lead to both lateral color and chromatic focal shifts for the LOWFS. Chromatic aberrations are uncorrectable with a deformable mirror, but the lateral color can be minimized by introducing a small wedge angle to the second surface of the interferometer pick-off dichroic (on the order of tenths of a degree). This wedge angle and the dichroic itself will introduce astigmatism in the wavefront of the LOWFS beam, which can be removed by the DMs located on each LOWFS optical path (see KAON 551, Wavefront Sensor System Design Report).

The acquisition camera will also be used during interferometer observations. The insertion of the dichroic causes spot sizes over J and H bands (observed simultaneously) on the acquisition camera to increase to 10 mas at the edges of the field. This is a small effect compared to the $\frac{120 \text{ arcsecond}}{1024 \text{ pixels}} = 117$ mas pixels on the acquisition camera detector.

The matched OAPs used in the first relay give excellent performance over a wide field at infinite conjugate. The values given in Table 1 indicate the maximum wavefront error and RMS spot radius over the 120 arcsecond field of patrol. The woofer mirror was deformed to provide excellent performance across the entire field, but even with a flat woofer mirror the first relay gives diffraction-limited performance over the entire 120 arcseconds. Additionally, each LOWFS path will have its own deformable mirror for correction at each natural guide star direction.

Table 3 Performance of the LOWFS in simultaneous J and H bands

Instrument (mode)	λ (μ)	F/#	FOV ″	Fld curv. (mm)	RMS WFE (nm)	RMS Spot Radius (μ)	RMS Spot Radius (milli-″)	Airy radius (μ) at 1.17μ	Lateral color (μ)	Chrom. Focal shift (μ)	Depth of focus (mm)
LOWFS	**1.17-1.78**	**13.66**	**120**	**1200**	**35**	**4**	**5.5**	**19.5**	**0**	**0**	**0.9**
LOWFS with interferometer	**1.17-1.78**	**13.66**	**120**	**1200**	**45**	**5**	**7**	**19.5**	**1.3**	**91**	**0.9**

4.2 Science Instruments, Narrow-field Relay

As explained in section 3.6, the narrow-field relay passes a rectangular 40x60 arcsecond field of view, the central 40x40 arcseconds of which are intended for science observations. It consists of two unmatched OAPs resulting in an increase of focal ratio to f/41. The larger focal ratio results in an image scale of 2.18mm/arcsecond at the focal plane, and an Airy radius of 50μ (23 milli-

arcsecond) at 1μ wavelength. The science instrument is intended to cover a wavelength range from z-band (0.8 μ) to K-band (2.4μ).

In optimizing the second relay science path with the deformable mirrors, the correction applied to the woofer DM when evaluating the LOWFS in section 4.1 also provided the best correction over the field in the second relay. The aberrations resulting from the non-matching pair of OAPs in the second relay are strongly field dependent, so a correction applied to the tweeter DM does not result in better performance over the whole field.

When the science instrument is used with the NGS WFS dichroic in place, a very small amount of chromatic aberration results. The NGS WFS has been designed with a small wedge (0.4°) angle on the second surface to minimize lateral color over the entire wavelength range. The astigmatism the NGS WFS dichroic produces is easily corrected by the tweeter DM, but will not be seen on the NGS WFS and so will need to be measured through another means (image sharpening, etc.).

Table 4 Performance of the narrow-field relay with the NGS dichroic in place.

Observing band	λ (μ)	F/#	FOV ″	Fld curv. (mm)	RMS WFE (nm)	RMS Spot Radius (μ)	RMS Spot Radius (milli-″)	Airy radius (μ)	Lateral color (μ)	Chrom. Focal shift (μ)	Depth of focus* (mm)
z-band	**0.85-1.05**	**46**	**40**	**300**	**25**	**22**	**9**	**48**	**2.9**	**28**	**6.8**
Y-band	**0.97-1.07**	**46**	**40**	**300**	**25**	**22**	**9**	**55**	**0.7**	**11.8**	**8.4**
J-band	**1.17-1.33**	**46**	**40**	**300**	**25**	**22**	**9**	**66**	**1.2**	**17**	**10**
H-band	**1.49-1.78**	**46**	**40**	**300**	**25**	**22**	**9**	**84**	**1.9**	**34**	**13**
K-band	**2.03-2.37**	**46**	**40**	**300**	**25**	**22**	**9**	**115**	**2.9**	**53**	**18**
NGS	**0.6-1.0**	**46**	**40 patrol**	**300**	**24**	**22**	**9**	**34**	**0**	**0**	**3.5**

The NGS WFS focal plane encounters only reflective optics, so does not suffer from chromatic aberrations. The analysis above does not include the effects of atmospheric dispersion or an atmospheric dispersion corrector which will be required in the science instrument's beam path, nor does it include the effects of the entrance and exit windows to the AO enclosure.

Figure 8 shows the degradation of the optical performance with field angle, due to the unmatched OAPs used in the second relay. Figure 8 shows an example of the spots at the on-axis, mid, and extreme field angles of the science instrument.

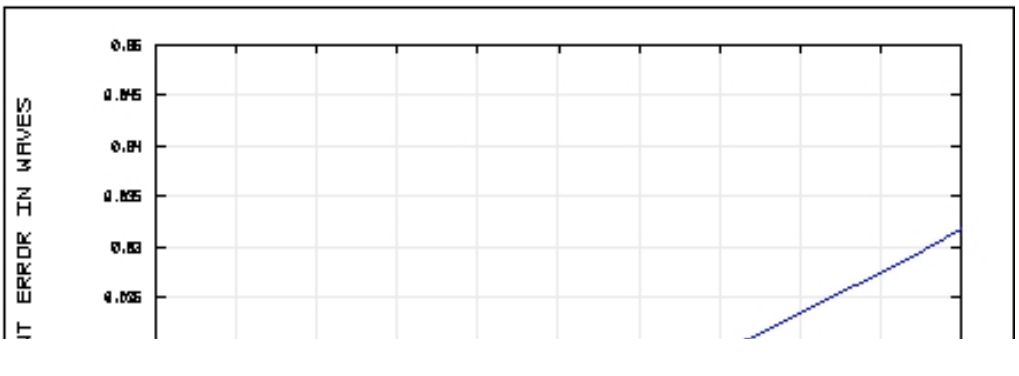

Figure 8 WFE as a function of field at the output of the second relay. Field size is 40 arcseconds diameter. Wavelength is 1μ.

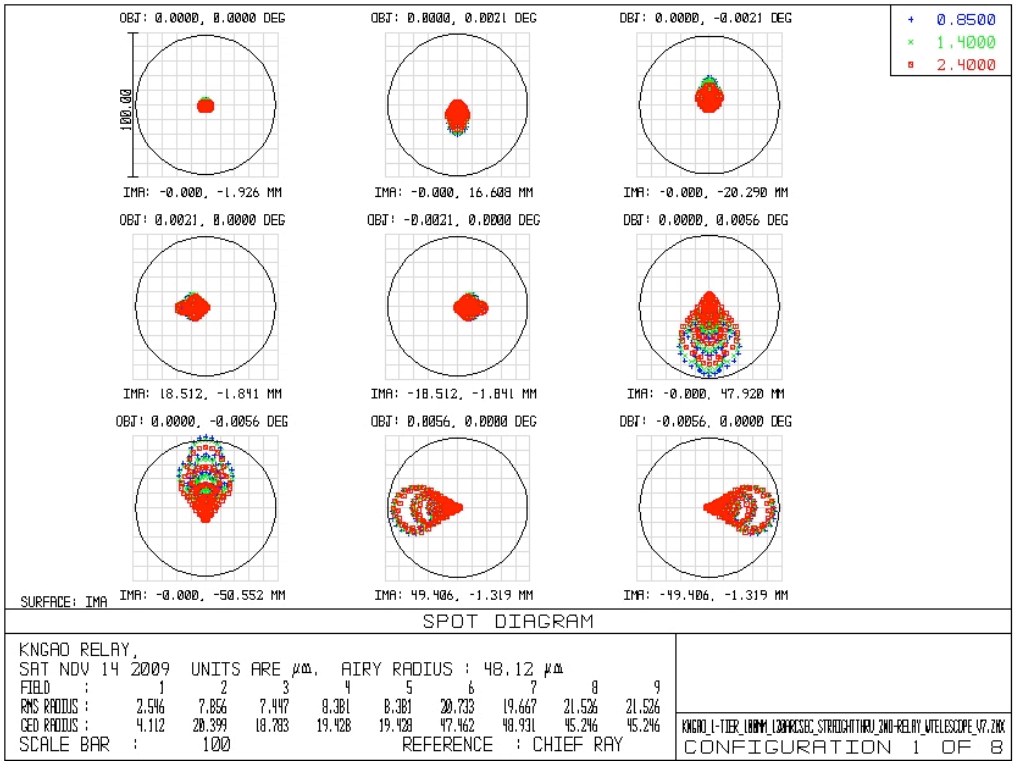

Figure 9 Spots at the focal plane of the second relay. Extreme field points correspond to a 40 arcsecond diameter field.

4.3 Laser Guide Star Wavefront Sensor (LGS WFS)

The LGS WFS dichroic pick-off lies in the collimated space between the woofer DM and OAP2. The laser guide stars, over a 120 arcsecond diameter patrol field, are re-imaged using a 1-glass biconvex lens with a parabolic convex surface. Because the relay passes only 589 nm sodium light, chromatic aberrations are not an issue. This lens was optimized for 90km (the spot size varies by only 10s of milliarcseconds between 90 and 180km). Table 5 details the performance of the LGS WFS relay. The focal plane of the LGS WFS is tilted by 4 degrees and has negligible field curvature (compared to the astigmatism present at the far off-axis field points).

Values quoted in Table 5 are at the edges of the field, and thus represent the worse case performance. Figure 10 displays the RMS wavefront error as a function of field. Figure 11 shows spot diagrams on-axis and at extreme field positions.

Table 5 Performance of LGS WFS

Conjugate height	FOV, arcsec	Field Curvature (mm)	RMS WFE (μ)	RMS Spot Radius (milli-arcseconds)
90km	120	883.205*	1.4	233
180km	120	>2000*	1.6	265

* The effects of these field curvature values are negligible compared to the effects of astigmatism at the extreme field points.

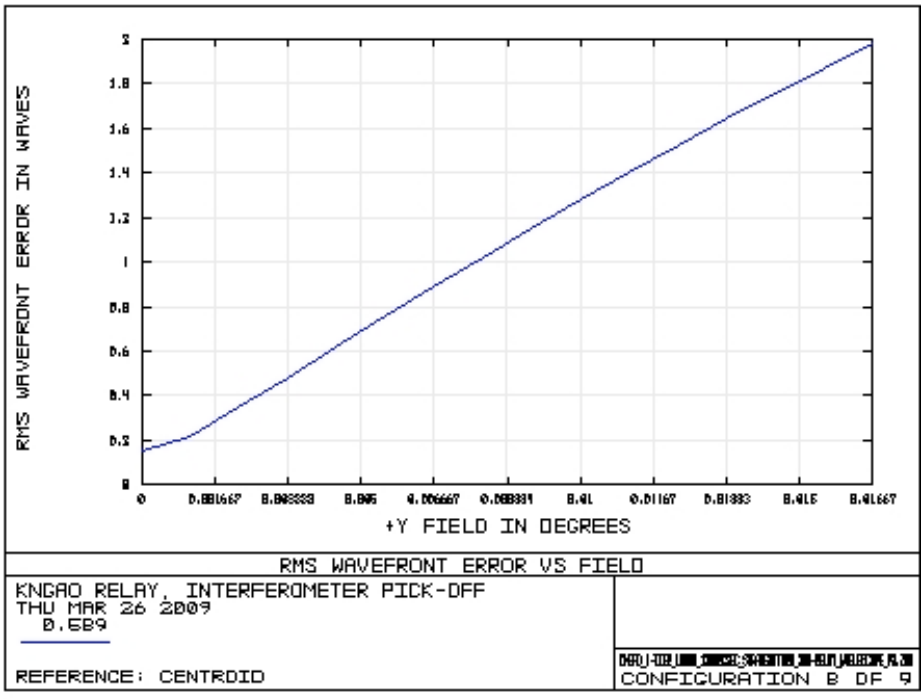

Figure 10 WFE as a function of field at the LGS WFS. Wavelength is 0.589μ, observations at zenith (distance is 90km). Field is 120 arcseconds in diameter.

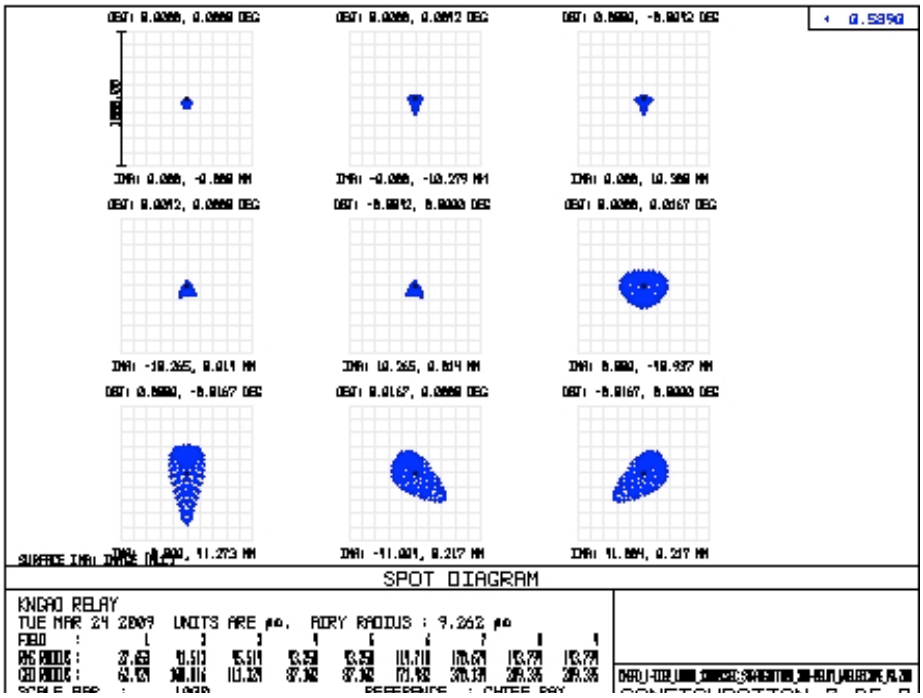

Figure 11 Spots at the focal plane of the LGS WFS. Wavelength is 0.589µ, observations at zenith (distance is90km). The spots on the edge of the 120 arcsecond diameter field are roughly 235 milliarcseconds on-sky.

To determine whether this amount of laser guide star wavefront aberration is acceptable requires further analysis. As seen in Figure 11, the spot size of the laser guide stars produced by the OAP/bi-convex relay is roughly 250 milli-arcseconds at the edges of the 120 arcsecond diameter field. According to KAON 551, WFS sub-system conceptual study report, this compares to other factors as follows: diameter of point source laser at Na layer, 1.08 arcseconds; seeing, 470 milli arcseconds; elongation, 850 milli-arcseconds; diffraction limit of subaperture, 660 milli-arcseconds. The relay static aberration contribution to spot size is smaller than all of these, and is much smaller than the combined 1.47 arcsecond expected laser guide star size. The error budget shown in KAON 551, Table 2, allows a 250 milliarcsecond spot size "due to aberrations in AO thru to WFS". It's not clear whether this includes contributions from the WFS optics. This requirement needs clarification. The current design meets this requirement.

Another concern is the effect of the wavefront error on the dynamic range of the Shack-Hartmann wavefront sensors. The static aberration will cause movement of the Hartmann spots from the centers of the subapertures. If the static aberrations cause the Hartmann spots to move a significant fraction of a subaperture, that subaperture will be compromised in its dynamic range. To evaluate the extent of this problem, the position of the Hartmann spots in the subaperture, due to static aberrations, were evaluated in three ways: through Zemax modeling of the LGS WFS, a simplified analytic approach, and through computer modeling of the Hartmann sensor.

In Zemax the wavefront sensors were modeled using non-sequential components. Each field point encountered its own collimating lens, which imaged the telescope pupil onto a lenslet array. The resulting Hartmann pattern allowed visual inspection of the placement of the Hartmann dots, given the static aberrations at each field point. Figure 12 shows no gross Hartmann spot displacements on an 18x18 subaperture grid. The 64x64 subaperture grid specified for NGAO is difficult to model in Zemax, due to computation time.

Figure 13 shows an approximate calculation of the spot displacements given the wavefront errors in the extreme field points. The static aberrations consist mostly of astigmatism, and analysis in Zemax indicates about 9 microns peak-to-valley of astigmatism is present in the extreme field positions. This corresponds to Hartmann spot displacements of approximately 6% of the subaperture.

Finally, a Hartmann sensor simulator developed by Mark Ammons and Don Gavel of the LAO was used to assess the spot movement. Again, the static aberrations were assumed to be astigmatism with an approximate magnitude of 9 microns peak-to-valley. This wavefront phase error, modeled as a Zernike polynomial with coefficients corresponding to pure astigmatism, was propagated through a 64x64 subaperture lenslet array, and the resulting centroid shifts were measured. The model assumes Fresnel propagation to the lenslet array focus. Figure 14 shows an example of one pupil edge of the Hartmann sensor, with the subaperture boundaries drawn in and the shift of the Hartmann spots due to astigmatism visible. The center of mass centroiding results shown in Figure 15 predict shifts of approximately 5-6% of a subaperture, consistent with our analytic calculations in Figure 13.

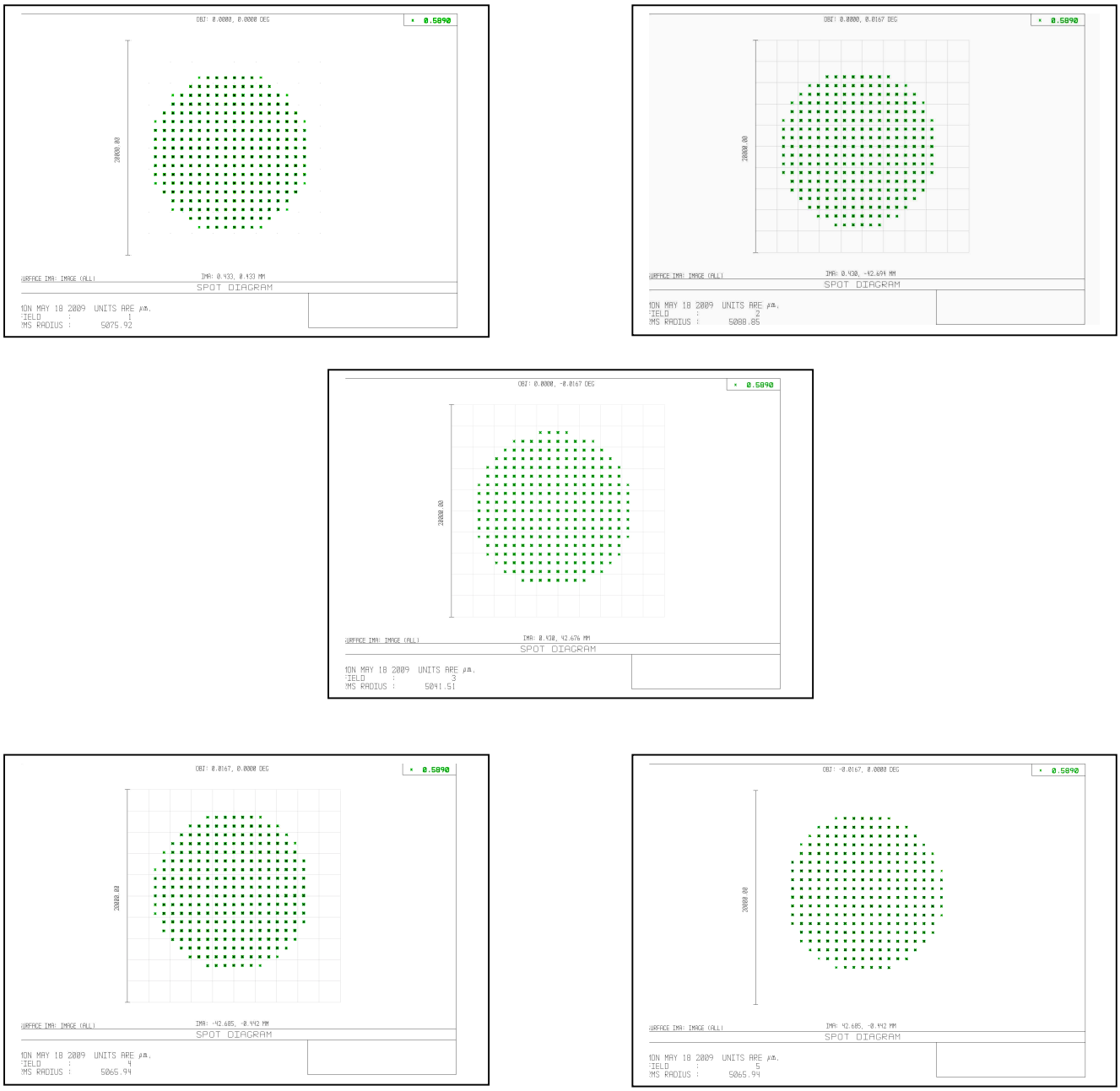

Figure 12 Zemax modeling of the on-axis (top, left) and extreme x and y field positions (120" diameter field of view) LGS WFS. For each field position, a separate f=180mm collimator lens imaged a pupil on an 18x18 subaperture lenslet arrays. The spot diagrams show the Hartmann spots produced by each of the lenslet arrays. Visual inspection shows no pronounced displacement of spots due to static aberrations in the LGS relay. An 18x18 subaperture lenslet array was assumed for ease of display and speed of computation.

LGS WFS Hartmann spot displacement due to static aberrations.

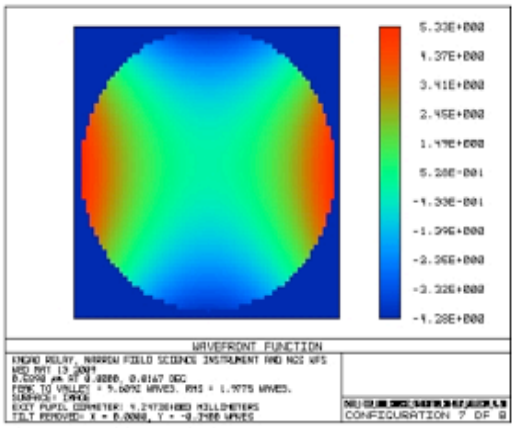

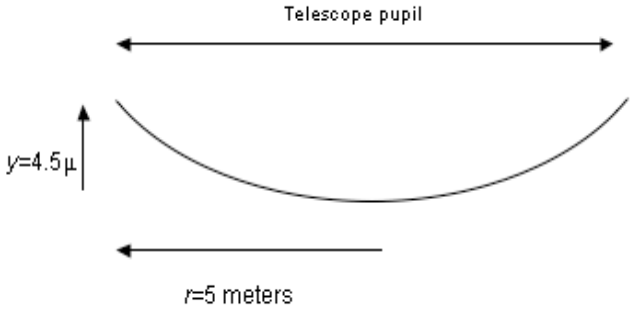

The wavefront error on the extreme field points of the LGS WFS is dominated by astigmatism.

Use the slope of thewavefront to determine the maximumspot displacementon the wavefront sensor:

$$y = ar^2 \rightarrow 4.5\times10^{-6}\,\mathrm{m} = 25\,\mathrm{m}^2 a$$

$$a = 1.8\times10^{-7}\,\mathrm{m}^{-1}$$

where y is the 0 to peak wavefront error across the pupil, and r = 5m is the pupil radius.

$$\frac{dy}{dr} = 2ar = 3.6\times10^{-7}\,\mathrm{m}^{-1}(5\mathrm{m}) = 1.8\times10^{-6}\ \text{radians}$$

$$= 0.37\ \text{arcseconds}$$

LGS WFS detector has 1.5 arcsecond pixels, 4x4 subapertures, so maximum spot movement is ~6% of a subaperture

Figure 13 Simple analytical treatment of Hartmann spot displacement due to static aberrations in LGS WFS optical path. The static aberrations at the extreme field points are dominated by astigmatism, as shown in the false color wavefront in the upper left. This will cause a Hartmann spot displacement of roughly 6% of a subaperture at the edges of the pupil.

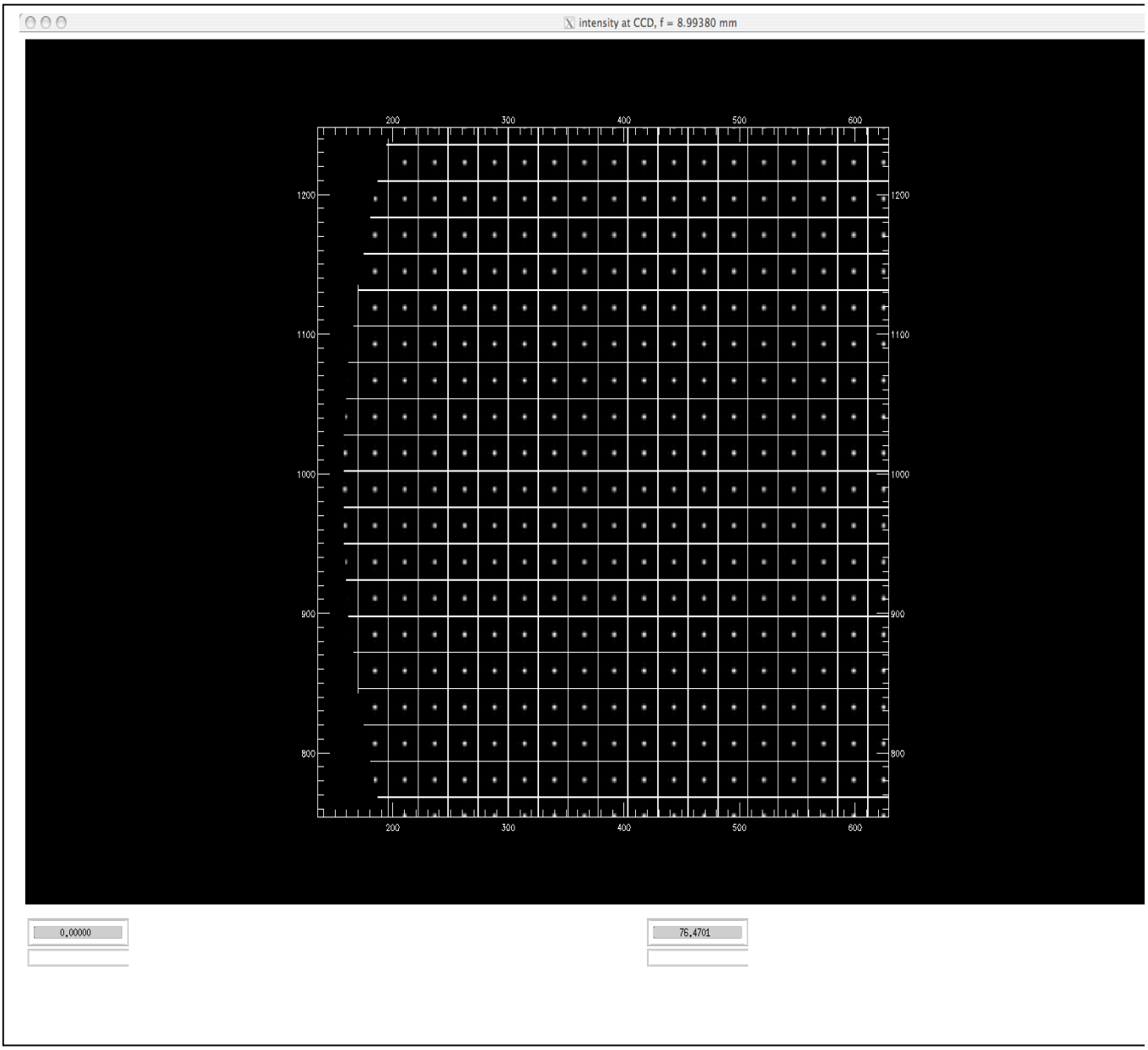

Figure 14 Results of a Hartmann sensor simulation given the static errors present in an extreme field of the laser guide star wavefront sensor relay. At 60 arcseconds radius, the wavefront entering the w sensor optics is expected to have as much as 9 microns peak-to-valley of predominantly astigmatism. extreme static aberration is due to the optical relay's optimization for objects located at infinity (natu stars), while the laser guide star varies between 90 and 180 km above the telescope. The image abov the location of Hartmann spots with respect to the subaperture grid, at one edge of the pupil.

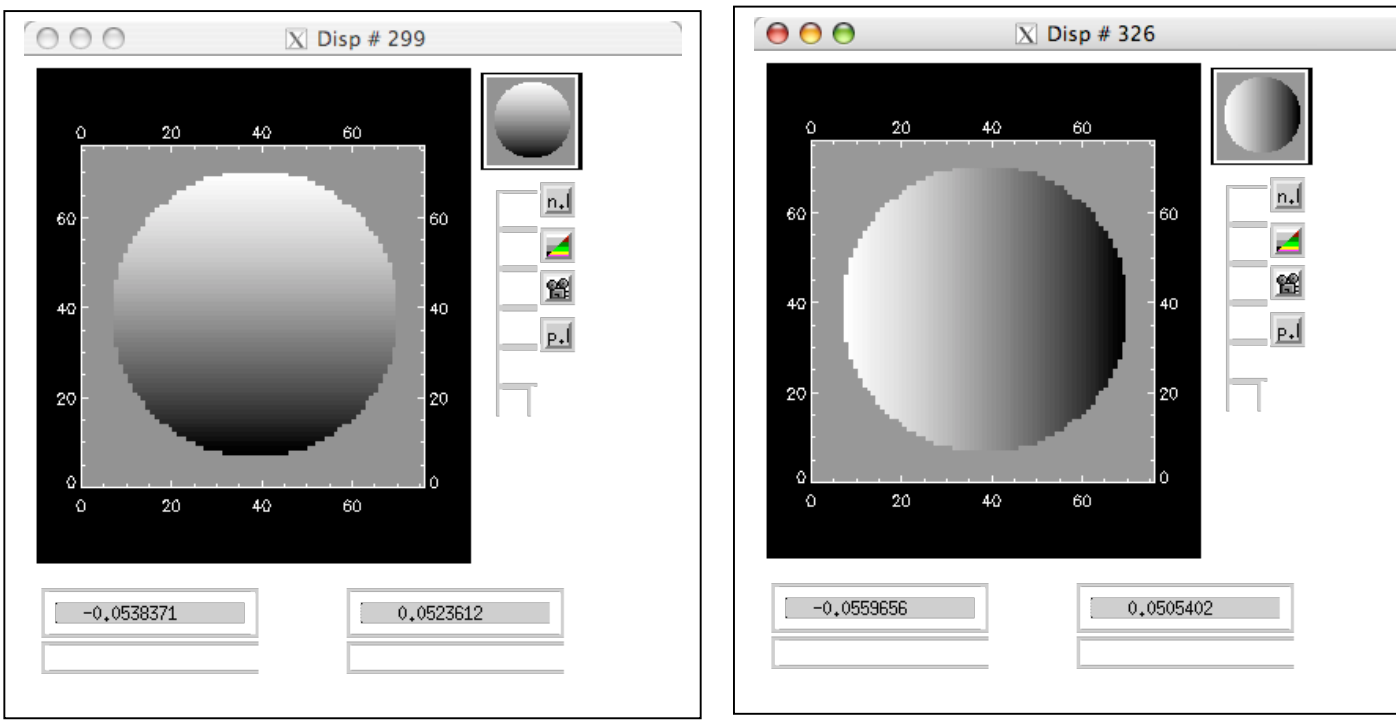

Figure 15 Given the Hartmann spot locations shown in Figure 12 over the entire pupil, centroids wer calculated and are displayed above, normalized to the subaperture width. X centroids (left) and Y-centroids (right) are displaced by static aberrations by approximately +/- 5% of a subaperture at the edges of the pupil.

4.3 Pupil Distortion on Deformable Mirrors

We have included Jim Bell's drawings of the mapping of the Keck telescope primary mirror on the woofer (Figure 16) and tweeter (Figure 17) deformable mirrors. The mapping includes the 10 degree incidence angle on both the mirrors. The woofer mirror in Figure 16 is the Gemini DM4.5 designed by CILAS. It's 22x22 actuators are on a 5mm pitch. The tweeter mirror in Figure 17 is the 64x64 MEMs device designed for the Gemini Planet Imager project. It's actuators are on 0.4mm centers.

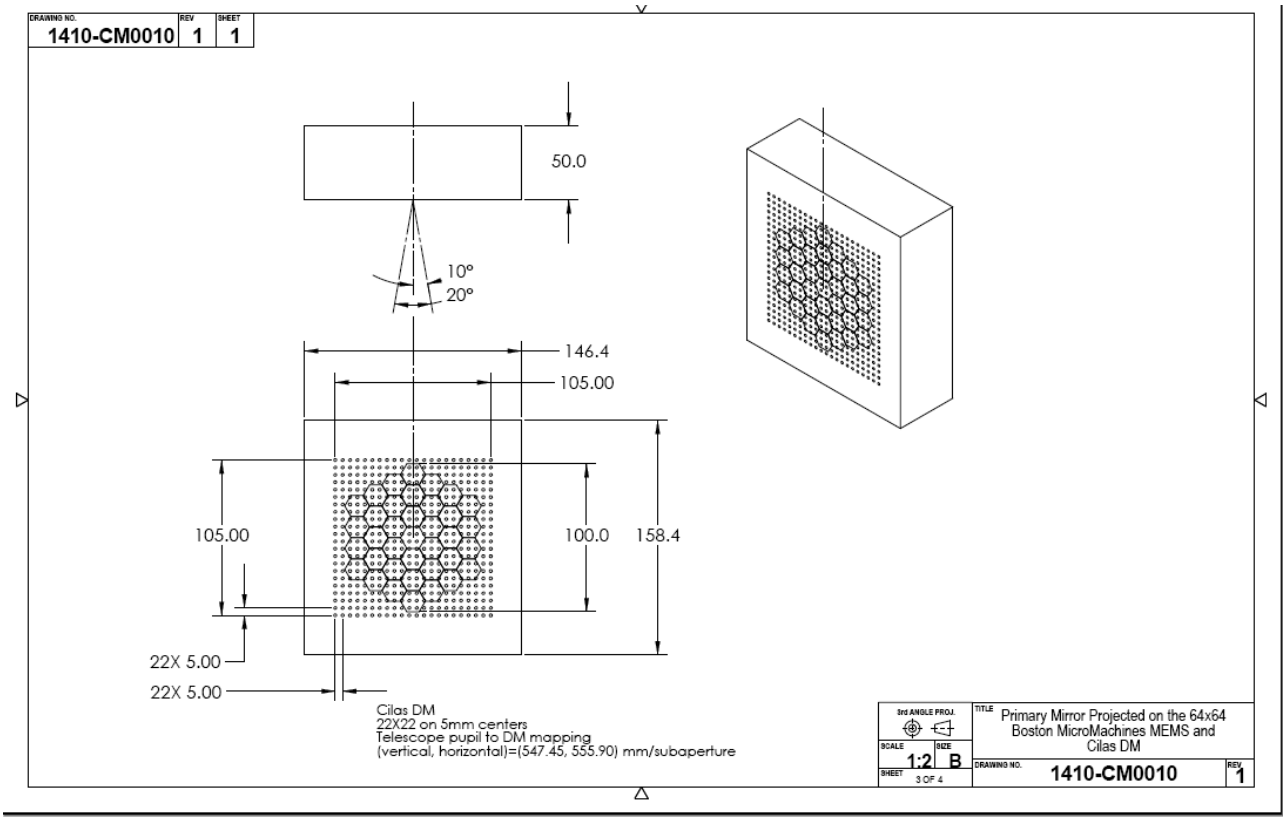

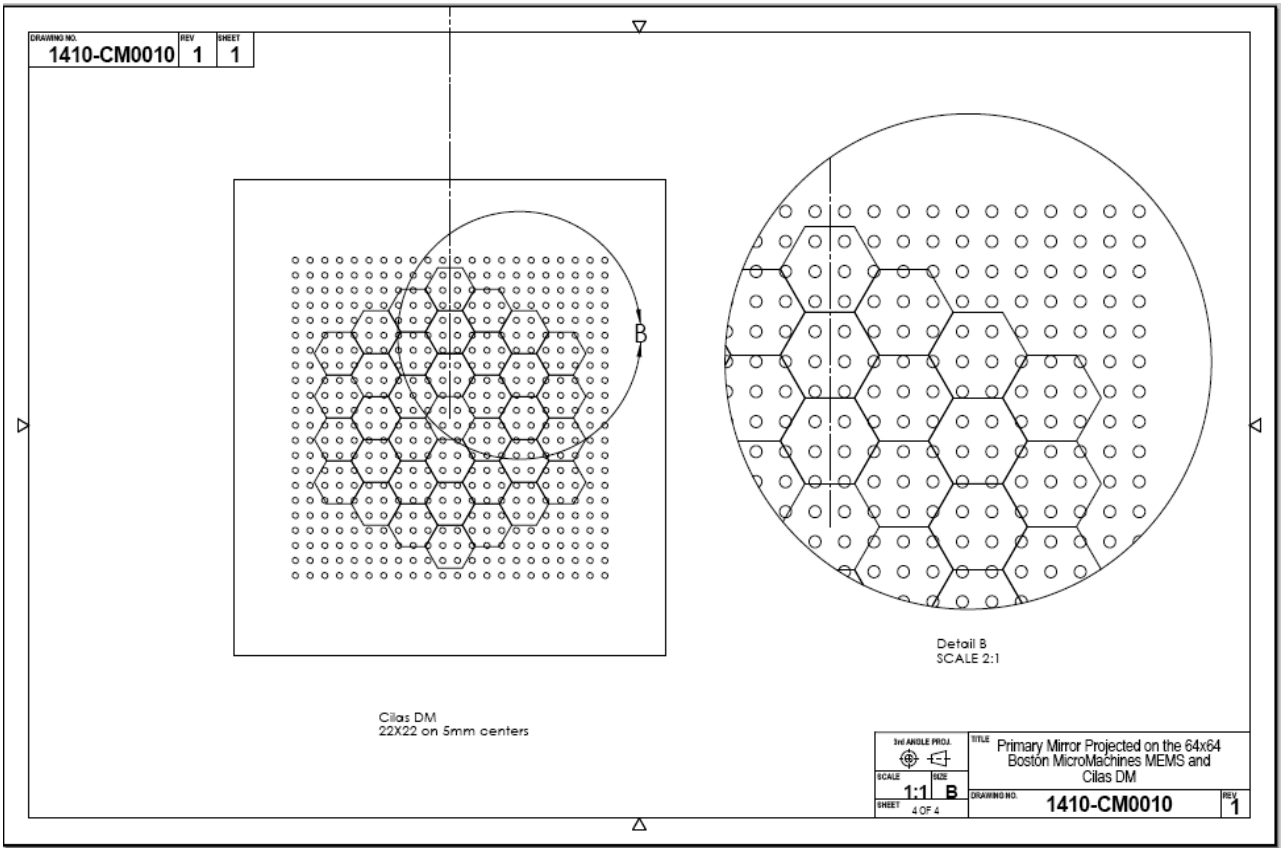

Figure 16 The 100mm pupil as mapped by the OAP on the woofer deformable mirror. The DM used in this drawing is the 22x22 actuator, 5mm pitch device designed for Gemini. Figure courtesy of Jim Bell.

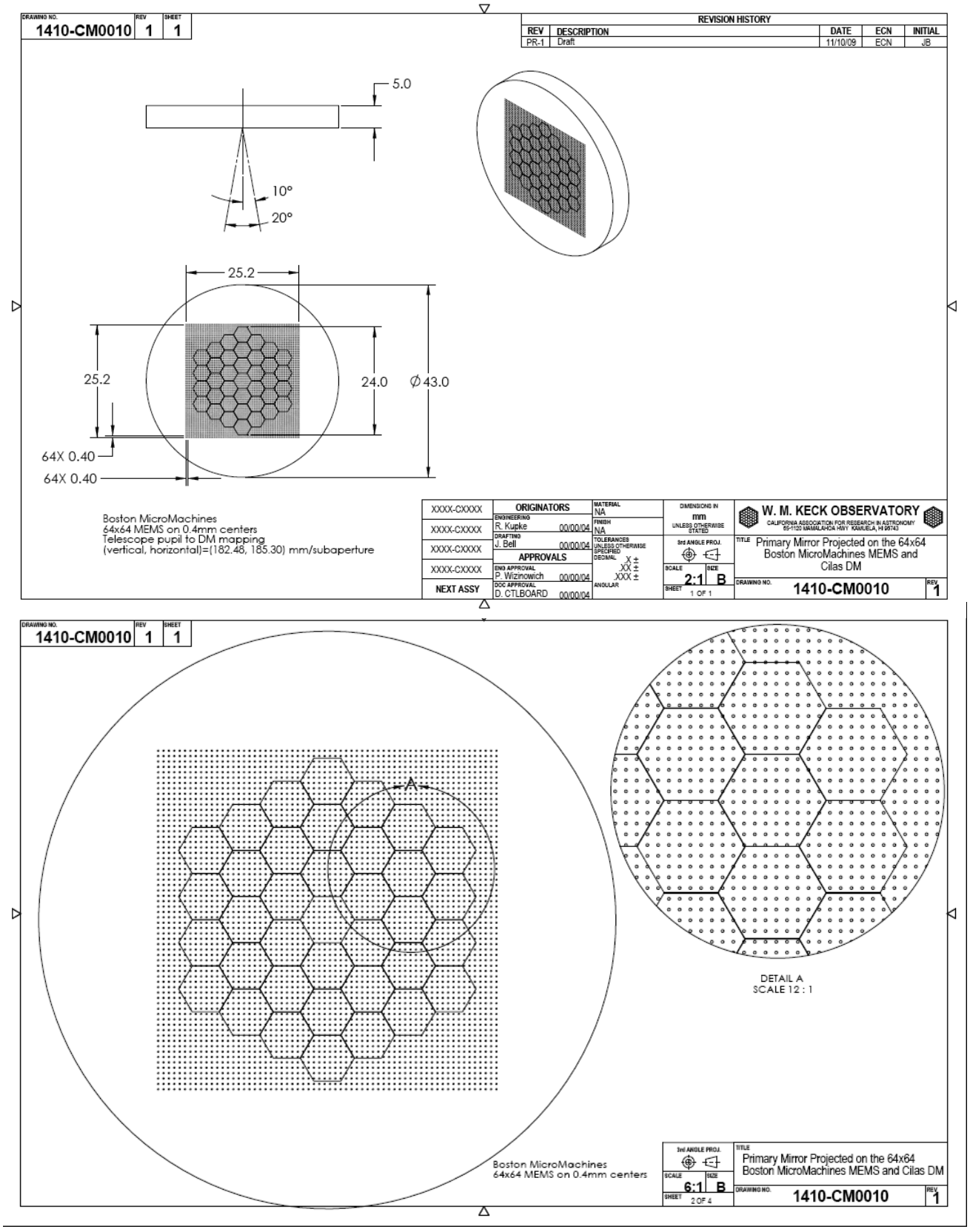

Figure 17 The telescope pupil, imaged on the tweeter DM by OAP3. The pupil image is 24mm in diameter, covering 60x60 actuators of the 64x64, 0.4mm pitch device. Figure courtesy of Jim Bell.

Pupil distortion in the NGAO relay manifests itself in at least three ways. The first is the degree to which a grid of points on the primary mirror maps to a demagnified, but square grid on the DM. Another consideration is the field-dependent pupil aberrations. This effect causes the chief rays from the various field angles to not all pass through the center of the pupil (paraxially, the chief rays all pass through the center of the pupil, by definition, but for real rays, this is not generally true). In other words, the pupil (i.e., the DM and the correction it applies to the wavefront) is shifted with respect to the telescope primary by an amount depending on the field angle—this is similar to anisoplanatism caused by atmospheric aberrations at an altitude not conjugate to the DM. Finally, a third effect is DM-to-lenslet misregistration and scale errors. This depends on the pupil re-imaging optics chosen for the wavefront sensors.

In the analysis, the telescope primary became the "object", and field points were defined on the edges of the primary mirror. Observed field angle was set by adjusting the "stop" size placed at the Nasmyth focus to accommodate a 120 arcsecond diameter field for the woofer, and a 40 arcsecond diameter field for the tweeter in the narrow-field relay. Results are shown in Table 6 and figures 18-21 on the following pages. Requirement FR-1505 specifies that the first relay shall have no more than 0.5% grid distortion at the pupil. As seen in Figure 18, the first relay exhibits 0.43% grid distortion at the woofer DM. Requirement FR1506 specifies that the second relay have no more than 0.2% grid distortion. Unfortunately, the relay design does not meet his requirement, as Figure 20 show, having a grid distortion of 0.26% at the MEMs DM. FR-1507 and FR-1508 require that the pupil aberrations be no more than a tenth of a subaperture in the first and second relays, respectively. The first relay meets this requirement. As seen in Figure 19, the image of the pupil on the deformable mirror produces 0.24mm FWHM spots when considering a 120" field. This is 5% of a subaperture. The second relay, however, does not meet the 10% requirement. It produces 0.06mm spots on the 0.4mm subaperture, or 15% of a subaperture when the science field of 40" is considered.

Table 6 also summarizes the pupil tilt and curvature on the woofer and tweeter DMs. FR-1510 and FR-1511 specify that the pupil tilt will be no more than 1 km on sky for the tweeter and 250m on sky for the woofer. We are well within these requirements.

Table 6 Characteristics of the pupil image on the deformable mirrors.

	Diameter (mm)	Field (″)	# actuators	Tilt (meters on sky, peak)	Curvature (mm)	Max Grid Distortion	Pupil PSF, (μ)
DM1, woofer	100	120	20x20	59	3000	0.4%	240
DM2, tweeter	25	40	64x64	225	328	0.26%	58

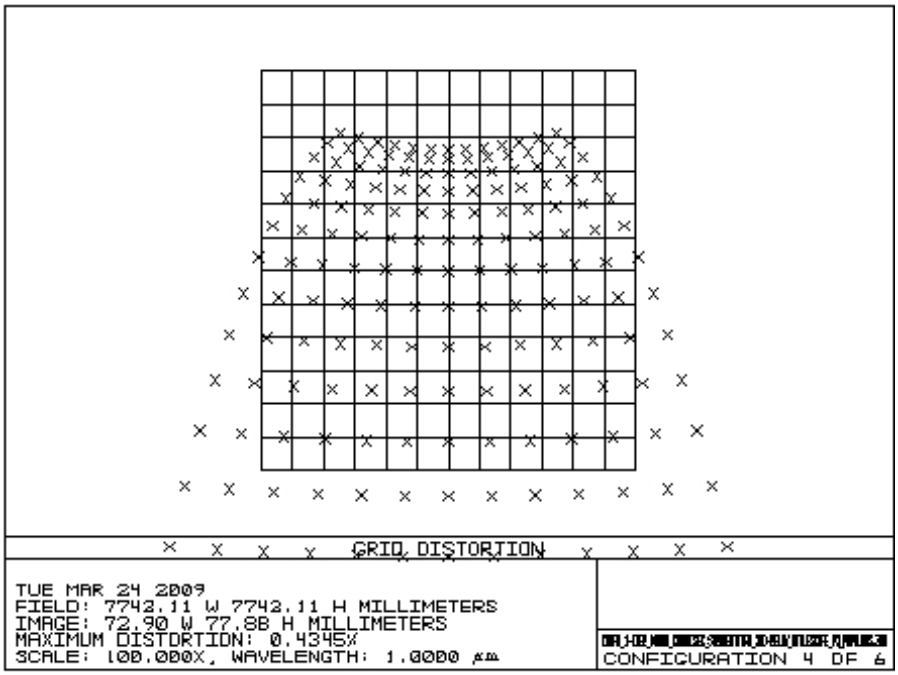

Figure 16 Grid distortion at the woofer mirror pupil location, magnified by a factor of 100 to emphasize shape.

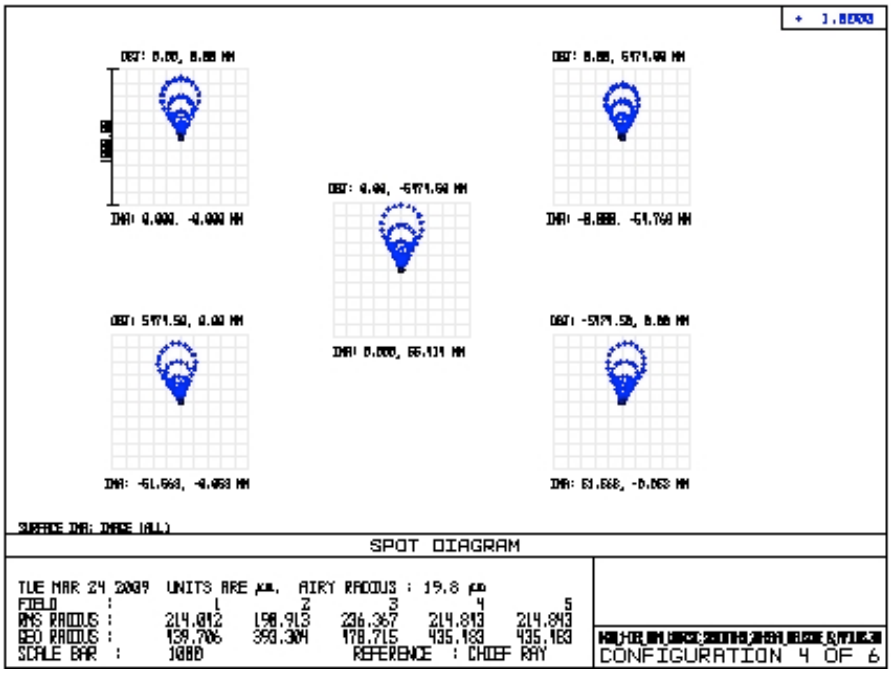

Figure 17 Spot diagrams for 5 places on the primary mirror, as imaged onto the woofer DM. Field considered is 120 arcsecond diameter. The chief rays from the on-axis field angles make up the point of the comatic pattern, while the chief rays for field angles of 60 arcseconds off axis make up the outer "radius" of points on the comatic pattern.

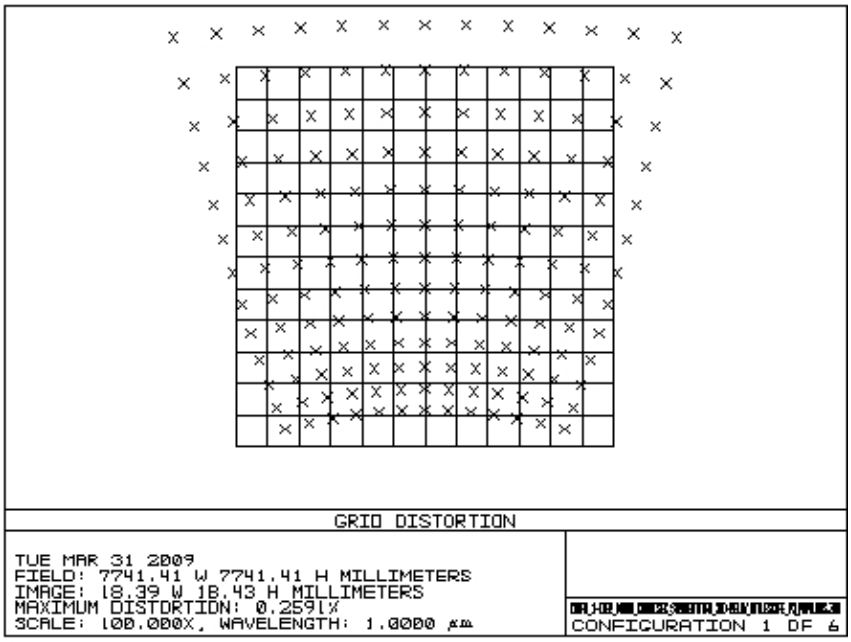

Figure 18 Grid distortion of pupil at 25mm DM. Scale is magnified 100x to emphasize shape of distortion. Maximum distortion is 0.26%.

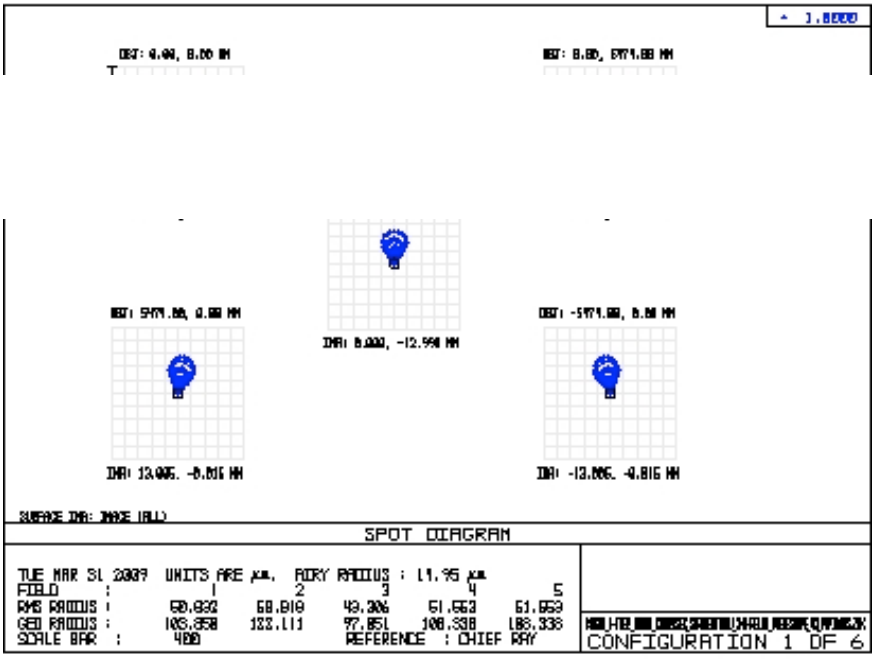

Figure 19 Spot diagram for 5 places on the primary mirror, as imaged onto the 25mm DM. Field considered is 40 arcseconds diameter.

4.4 Telecentricity

Three of the outputs of the relay require the exit pupil of the relay to be located at infinity. The Zemax EXPP (exit pupil position) operand unfortunately is not valid for decentered systems (Zemax manual, June, 2007, p442). To roughly check telecentricity a paraxial lens with a focal length of 200mm was added to the focal plane of each relay. A pupil at infinity will image at exactly 200mm from the paraxial lens. Figures 20, 21, and 22 show the re-imaged pupil planes of the LGS WFS relay, the LOWFS (first) relay, and the science (second) relay, respectively. The image of the pupil is the location where all the field points cross. In this way large deviations from telecentricity can be discovered.

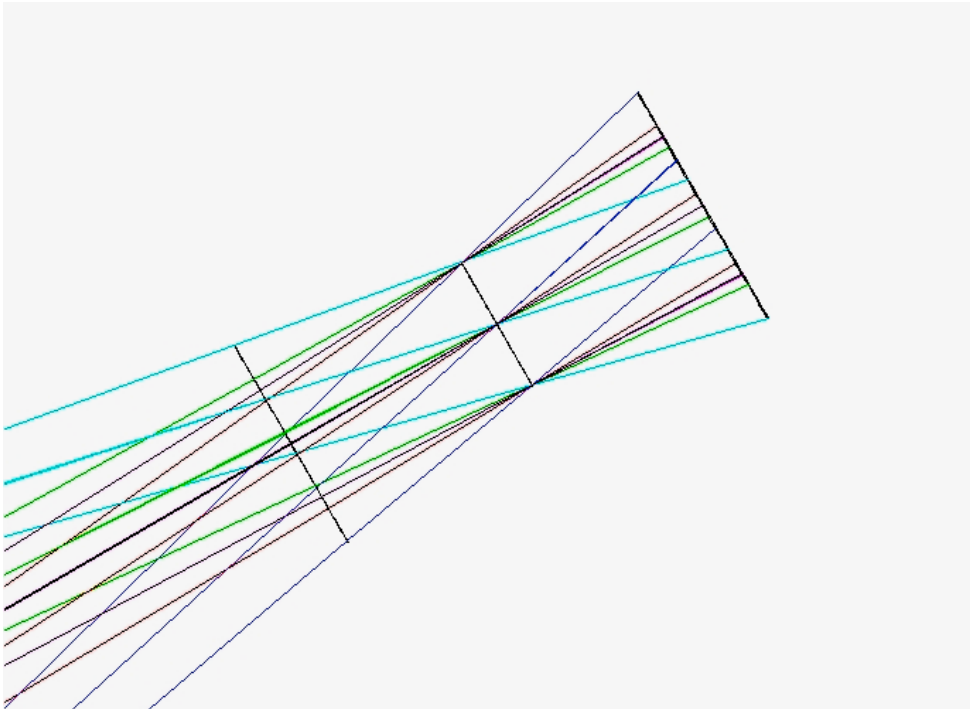

Figure 20 A paraxial lens has been placed at the focus of the LGS WFS relay. It produces a pupil image one focal length away (center line). For scale surfaces are placed 25mm before and after the focal length of the paraxial lens.

5. Optical Tolerancing

5.1 Introduction

Analysis of tolerances in the optical design is done with the Zemax EE tolerancing tool. The tolerances analyzed can be divided into two categories: mounting tolerances essential for the mechanical design and manufacturing tolerances important for the vendors producing the optics. Included in the mounting tolerances are the tilt and decentration of the optical elements, as well as distances between them. The manufacturing tolerances concern the radii of curvature (for the powered optics), flatness (for the flat mirrors and dichroics) and off-axis angles (OAAs). The telescope was not included in the tolerancing.

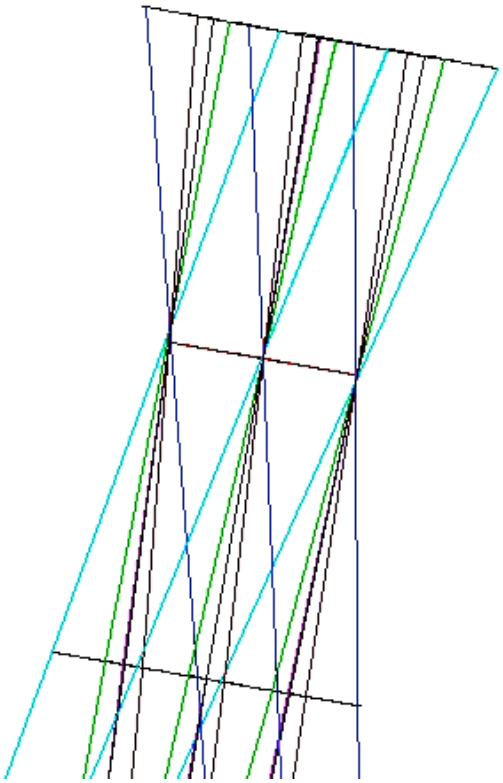

Figure 21 A paraxial lens has been placed at the focus of the LOWFS relay. It produces a pupil image one focal length away (center line). For scale surfaces are placed 25mm before and after the focal length

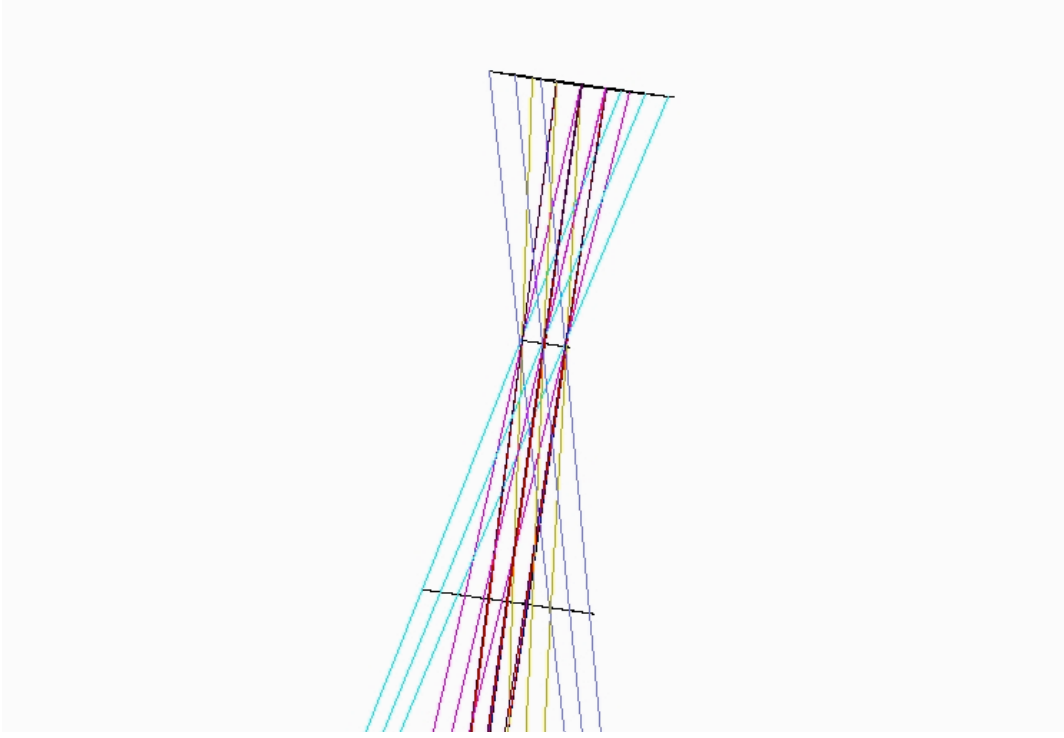

Figure 22 A paraxial lens has been placed at the focus of the science relay. It produces a pupil image one focal length away (center line). For scale surfaces are placed 25mm before and after the focal length

Zemax allows tolerances to be evaluated by several different criteria. We have chosen the RMS wavefront error merit criteria, as this is directly comparable to values in the derived error budget. We've also performed a boresight criteria analysis, to ascertain stability requirements for the optical mounts. The analysis was performed at 1 micron wavelength. Because of the difficulty in performing tolerance analyses on multi-configuration operands, the Zemax file was reduced to the science path configuration only (figure 6). Tolerances may also be performed separately on the LGS WFS optical path, and the LOWFS, first relay if desired.

Compensators may also be defined in Zemax, and boundary values defined for the compensators. For these analyses we allowed compensation of the back focal distances of the first and seconds relays, with the boundary condition of +/- 10 mm. The compensators were optimized using orthogonal descent.

Initially, we performed a sensitivity analysis in which the change in merit criteria (RMS wavefront error or boresight) is calculated for each tolerance individually. This allows evaluation of the "worst offenders", indentifying which tolerances must be tightened, and which can be relaxed. An aggregate performance is estimated by a root square sum (RSS) calculation.

Once reasonable tolerances are determined using the sensitivity analysis, a Monte Carlo analysis simulates the effect of all the tolerance perturbations simultaneously. Zemax does this by assuming a normal distribution (modified Gaussian) of tolerance values within the user defined range of the tolerances. To provide adequate statistics, the Monte Carlo analysis was permitted to run n^2 times, where n is the number of individual tolerances.

5.2 Mounting Tolerances

Assembly tolerances resulting in acceptable performance of the NGAO relay are listed in Table 7. These tolerances are typical of standard assembly methods, and will not require extraordinary efforts to achieve.

Table 7 Mechanical tolerance values used in Zemax.

Parameter	Value	Units
Thickness (TTHI)	±0.200	mm
Decentration (TEDX/Y)	±0.100	mm
Element Tilt (TETX/Y)	±0.004	degrees

Thickness tolerances were applied to distances between optical elements, decentration was applied to OAPs, and tilt tolerances were applied to every optical element, including the OAPs, the DMs, the fold mirrors, and the dichroic beamsplitters.

The tilt and decenter of the K-mirror's individual mirrors, and the K-mirror unit as a whole, were included for completeness. However, the alignment and tolerancing of the K-mirror assembly, as it pertains to both pupil and image motion, has been analyzed in detail by previous generations of

Keck optical engineers. This analysis is still pertinent, as the distance of the mirrors to focus is similar to the existing system (especially when compared to the 20 m distance to the exit pupil). The subaperture width decreases by a factor of 64/20, and thus the tolerances to keep the pupil wandering less than 10% of a subaperture will be tighter by a factor of 3.2.

The sensitivity analysis indicates that the worst offenders are tilt errors in the woofer DM (not surprisingly) and OAP mounts. However, a tilt of 0.004 degrees (14.2 arcseconds) at OAP1 results in less than a nanometer additional RMS wavefront error. Table 8 summarizes the worst offenders that had an appreciable effect on the RMS wavefront error.

Table 8 Worst offenders, mechanical tolerances

Tolerance	Value (degrees tilt)	Criterion (RMS WFE, nm, nominal 18.8)
TETY 19, woofer	0.004	22.1
TETY 19, woofer	-0.004	22.1
TETY 16, OAP1	-0.004	19.7
TETY 16, OAP1	0.004	19.7
TETY 27, OAP2	-0.004	19.7
TETY 27, OAP2	0.004	19.7

A Monte Carlo analysis of mounting errors leads to a similar conclusion. The nominal RMS wavefront error due to static aberrations for a perfectly aligned system is 18.8 nm (at 1 micron wavelength). For the tolerances listed in Table 7, a 2401 iteration Monte Carlo analysis predicts that 90% of the configurations will have less than 23.7 nm RMS wavefront error. This includes contributions from tilt error in the woofer DM mount (which in practice will be mitigated by its attachment to the tip/tilt stage).

A boresight analysis was also performed to ensure that mechanical tilts and decenters resulted in movement on the camera of much less than a tenth of a pixel.

5.3 Manufacturing Tolerances

Considered separately are manufacturing tolerances to be specified to the vendor during procurement. These include tolerances on the radii of curvature for the OAPs, off-axis angles for the OAPs, flatness of the fold mirrors and dichroics, and figure errors for the OAPs. The off-axis nature of the OAPs led to difficulties in defining Zernike figure errors (i.e. the TEZI tolerance operand) because Zemax centered these aberrations on the parent parabola. Thus the figure errors for the OAPs will be considered with an analytic approximation outside of Zemax.

Table 9 Manufacturing Tolerances

Parameter	Value	Units
Radius (TRAD)	0.5%	Unitless
Flatness (TFRN)	±0.200	Fringes
Off-axis angle (TPAR)	$\pm 3.5 \times 10^{-5}$	Degrees

Table 9 details the manufacturing tolerances used in the Zemax analysis. The radius of curvature was assigned a tolerance of 0.5% of the radius, as given by Space Optics Research Labs (SORL) as a standard tolerance. The flatness of dichroics and folds was assumed to be within 0.200 fringes, as measured in a double pass Newton's rings type test. The off-axis angles (OAA) of the OAPs were given tolerances of 0.125 arcseconds, again as specified by Space Optics Research lab. The OAA tolerances were implemented by adjusting either the angle or off-axis distance in the coordinate break preceding the OAP surface. Chief ray solves were left in during tolerancing to ensure that off-axis angles and off-axis distances were consistent.

The worst offenders were OAP tolerances for radii of curvature. Again, the nominal criteria for RMS wavefront error is 18.8 nm. A change of 0.5% in OAP1's radius of curvature corresponds to a 3 nm change in wavefront RMS. The back focal distances of relays 1 and 2 are allowed to change ±10mm in compensation. Table 10 summarizes the worst offenders that made an appreciable effect on the RMS wavefront error. If distance from Nasmyth focus to OAP1 had been allowed as a compensator (in effect, adjusting the position of the OAP to ensure that the optic produces a collimated beam) the criterion change is negligible. Likewise, for OAP3 if the distance from the 1st relay focus to OAP3 had been allowed as a compensator.

Table 10 Worst offenders, manufacturing tolerances.

Tolerance	Value	Criterion (RMS WFE, waves, nominal 18.8)
TRAD 16, OAP1	6.8 mm	0.0221
TRAD 16, OAP1	-6.8 mm	0.0204
TRAD 34, OAP3	-1.75 mm	0.0189

A Monte Carlo simulation of manufacturing tolerances shows that these tolerances, like those adopted for mechanical mounting, are acceptable in terms of degradation to image quality. The 256 iteration Monte Carlo predicts that 90% of configurations will produce less that 20.5nm RMS wavefront error. The compensators in the Monte Carlo run had standard deviations which were 0.2% and 0.4% of the 1st relay back focal distance and 2nd relay back focal distance, respectively.

6. Work remaining for PDR

At the time of the mini-review, November 17, 2009, there are some aspects of the design and this document that are not complete for PDR. The science instrument ADC requires an evaluation of the linear and counter-rotating types of ADCs in context of required wavelength range and throughput. OAP wavefront error manufacturing tolerances have not been specified (as they cannot be accomplished with the Zemax tolerancing tool). A section on alignment of the AO relay will be included in the PDR. Specification of coatings for the optics and windows are not yet complete. Polarization analysis of the system as it pertains to the interferometer will need to be performed.